PHYSICAL REVIEW C VOLUME 53, NUMBER 6 JUNE 1996

High-multiplicity lead-lead interactions at 158 GeV/c per nucleon

P. Deines-Jones,[1] M. L. Cherry,[1] A. Dabrowska,[2] R. Holynski,[2] W. V. Jones,[1] E. D. Kolganova,[3] D. Kudzia,[1] B. S. Nilsen,[1] A. Olszewski,[1] E. A. Pozharova,[3] K. Sengupta,[1,*] M. Szarska,[2] A. Trzupek,[2] C. J. Waddington,[4] J. P. Wefel,[1] B. Wilczynska,[2] H. Wilczynski,[2] W. Wolter,[2] B. Wosiek,[2] and K. Wozniak[2]

[1]*Louisiana State University, Baton Rouge, Louisiana*

[2]*Institute of Nuclear Physics, Krakow, Poland*

[3]*Institute of Theoretical and Experimental Physics, Moscow, Russia*

[4]*University of Minnesota, Minneapolis, Minnesota*

(Received 28 December 1995)

The Krakow-Louisiana-Minnesota-Moscow Collaboration (KLMM) has exposed a set of emulsion chambers with lead targets to a 158 GeV/c per nucleon beam of ^{208}Pb nuclei, and we report the initial analysis of 40 high-multiplicity Pb-Pb collisions. To test the validity of the superposition model of nucleus-nucleus interactions in this new regime, we compare the shapes of the pseudorapidity distributions with FRITIOF Monte Carlo model calculations, and find close agreement for even the most central events. We characterize head-on collisions as having a mean multiplicity of 1550 ± 120 and a peak pseudorapidity density of 390 ± 30. These estimates are significantly lower than our FRITIOF calculations. [S0556-2813(96)00106-9]

PACS number(s): 25.75.Gz, 12.38.Mh, 24.85.+p

I. INTRODUCTION

Current interest in studies of relativistic heavy nucleus collisions is based on the expectation that fundamentally important physical phenomena may occur as a result of the formation of high-density, high-temperature nuclear matter. Under such extreme conditions, matter may undergo a transition into a deconfined quark-gluon plasma phase [1]. The required conditions may have existed in the early universe, and they may be created in the interiors of neutron stars and in central collisions of energetic heavy ions. This last possibility provides an opportunity to study such extreme conditions in terrestrial laboratories. If high-multiplicity lead-lead central collisions are characterized by sufficiently high transverse momenta $p_{t\pi}$ and central pseudorapidity densities $dN/d\eta$, the energy densities may reach the level at which a quark-gluon plasma (QGP) could be formed [2]. Although the produced particle multiplicities and their space angle distributions will surely be dominated by common features that reflect kinematical constraints and variations in the impact parameter, new phenomena (if they exist) may be observable above this anticipated background in forms such as very large multiplicities, nonstatistical variations, or fluctuations in the distributions of the secondary particles.

In December 1994, ^{208}Pb ions were accelerated at CERN to a momentum of 158 GeV/c per nucleon, by far the highest-energy ultraheavy nucleus beam ever produced. The Krakow-Louisiana-Minnesota-Moscow collaboration (KLMM, CERN experiment EMU-13) exposed a series of nuclear emulsion chambers with Pb targets to this beam in order to study charged particle multiplicities and angular distributions from interactions in the symmetric lead-lead system. Emulsion's excellent spatial resolution allows accurate track counting and angular measurement, with relatively small systematic uncertainties. In this paper, we present the first results from the measurement of a sample of 40 of the highest-multiplicity Pb-Pb collisions. In this analysis we consider only the gross properties of the angular distributions and the multiplicities. However, individual event multiplicities are sufficiently high in these collisions that it is now possible to search individual events for deviations from the behavior expected from models based on incoherent superpositions of nucleon-nucleon collisions. The investigation of fluctuations and the study of individual events will be subjects of a future study.

II. EXPERIMENT AND ANALYSIS PROCEDURES

The emulsions were exposed perpendicular to the beam in chambers of 20 emulsion plates each, spaced out over a distance of approximately 17 cm from the first Pb target to the final emulsion plate. Each emulsion plate consisted of a 200 μm thick acrylic base coated with a 55 μm Fuji ET7B emulsion layer on each side. An emulsion chamber is an extremely "light" detector, as each plate consists of only ~ 0.06 g/cm^2 of material. (Most tracks are measured before they pass through four such plates.) Each of the 32 chambers had a 10 cm $\times$5 cm front area, and held three to four 100 μm thick lead target foils. The exposure of the chambers to the beam resulted in an average of ~ 350 primary Pb ions/cm^2 across the face of the chambers, concentrated in three 1.5×2 cm^2 beam spots. This density was small enough to ensure a low delta-ray background and to keep to an acceptably low level the number of events cut because a noninteracting primary was too close.

To select a sample of relatively central interactions, the emulsion plates directly below each target were visually scanned for high-multiplicity events. After the initial scanning selections were made, each event was examined in all the plates upstream of the interaction and rejected if the primary was noticeably less ionizing (approximately five charge units) than nearby Pb tracks or if the primary had suffered an

*Current address: Horizon Comp., 5 Lincoln Hwy, Edison, NJ 08820.

0556-2813/96/53(6)/3044(7)/$10.00

additional observable interaction. The plates adjacent to the target allowed rejection of interactions occurring in emulsion rather than in the lead target. The event was also examined downstream and rejected if the remnants of the projectile contained fragments noticeably heavier than alphas. (Only two events were rejected on this basis.) Events with nearby (60 μm) noninteracting primaries which might obscure secondary tracks were also rejected. These high-multiplicity events are as conspicuous in the emulsion as the Pb primaries themselves. Few if any of the very largest events are missed in scanning. However, the appraisal of multiplicity during scanning is very rough, and therefore we expect a gradual roll-off of scanning efficiency at low multiplicities. Events with charge multiplicities above ~ 1000 are scanned efficiently, but those with lower multiplicities are sampled incompletely. The smallest scanned event has a multiplicity of 590. Scanning efficiency is discussed further in Sec. IV in connection with the multiplicity distribution.

As a result of the selection process, we have chosen events for analysis at a rate of $(1.42 \pm 0.18) \times 10^{-3}$ event per incoming primary. By using the parametrization of the charge-changing cross section for ultraheavy ion interactions found by Nilsen *et al.* [3] and Geer *et al.* [4], we expect a nuclear charge-changing cross section for 158 GeV/c per nucleon Pb-Pb interactions of 6.9 b. Using this calculated cross section, we estimate that we have selected $(22.2 \pm 2.7)\%$ of all nuclear charge-changing interactions in the lead targets of the scanned chambers.

To distinguish individual produced particle tracks emanating from a common vertex (i.e., the desired signal) from various backgrounds (delta rays, emulsion fog, emulsion surface imperfections, and particles from other events), one needs an image with micrometer resolution or better in all three dimensions, including depth. A charge-coupled device (CCD) camera-equipped microscope with stepper motors controlling all three microscope stage axes is used for this analysis. The acquisition is controlled by software which steps the focus vertically in 0.8 μm increments through the emulsion layer and automatically detects the surfaces of the emulsion to begin and end acquisition. Depending upon the exact emulsion thickness, approximately 20 frames are acquired in each focus sequence. The image analysis software [5] searches the focus sequence for a persistent series of dark pixels radiating out from a common vertex, while rejecting isolated dark grains and tracks which do not point back to the vertex. The track "darkness," a measure of the ionization density, is also recorded in order to distinguish minimum ionizing tracks from those of alphas and heavier projectile fragments.

Projectile fragments are expected to be confined to the very forward direction. Figure 1(a) relates the track darkness to the track emission angle θ, and shows a population of dark fragments mostly confined to a 2 mrad cone. Figure 1(b) shows the darkness distribution for individual tracks inside the forward 2 mrad cone, corresponding to pseudorapidity $\eta = -\ln[\tan(\theta/2)] = 6.9$. Two peaks can be seen corresponding to minimum ionizing particles and to heavier particles (mostly alphas). We have identified tracks within this 2 mrad cone with darkness less than 15 as minimum ionizing particles and tracks with darkness of 15 or more as fragments. The rms opening angle of the particles identified as

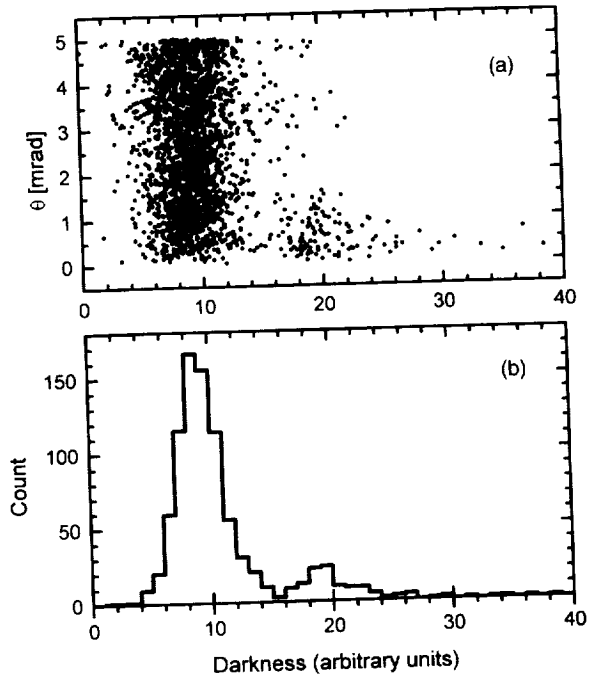

FIG. 1. (a) Track darkness vs opening angle θ. (b) Darkness distribution of all tracks in the forward 2 mrad cone.

fragments is ~ 0.7 mrad ($\eta = 8.0$).

Fields 108 μm$\times$140 μm across are digitized in an average of nine plates along the axis of the event, and successive measurements from the individual plate sides are then fitted together to reconstruct the tracks in the event. By comparing the reconstructed tracks to their constituent measurements, we have determined the imaging system's pair resolution to be 1.0 μm and the rms scatter of individual measurements within an emulsion layer to be 0.2 μm. To further discriminate secondary tracks from backgrounds, measurements in at least two emulsion layers are required within ~ 1.0 μm of each track [5]. This requirement results in the suppression of tracks below $\eta = 2.6$. All tracks in the data sample have been fully measured inside the $\eta \geq 2.9$ cone. In each event, the track detection efficiency and background rejection are estimated for each measured emulsion layer by counting the missing and rejected measurements in the successive plate sides, respectively. The image processing software detects tracks with an average 96% efficiency or better for $\eta \geq 2.6$. We have compared a sample of events reconstructed by the software track by track with manual measurements. These comparisons agree to within 5%.

In the transverse plane, the fitted track location has a statistical uncertainty of ~ 0.2 μm and tracks typically leave the field of view at transverse distances ~ 40 μm from the event axis; the resulting 0.5% uncertainty in the transverse position corresponds to $\delta\eta = 0.005$. A systematic uncertainty in the transverse positions derives from the absolute determination of the event axis. This is measured manually under the microscope by observing the positions of nearby noninteracting primary ions as reference tracks. The reference track positions are determined to 5 μm; over a typical distance of 3.3 cm (corresponding to 15 emulsion plates), this results in a typical systematic uncertainty of 0.15 mrad in the absolute positioning of the event with respect to the reference system.

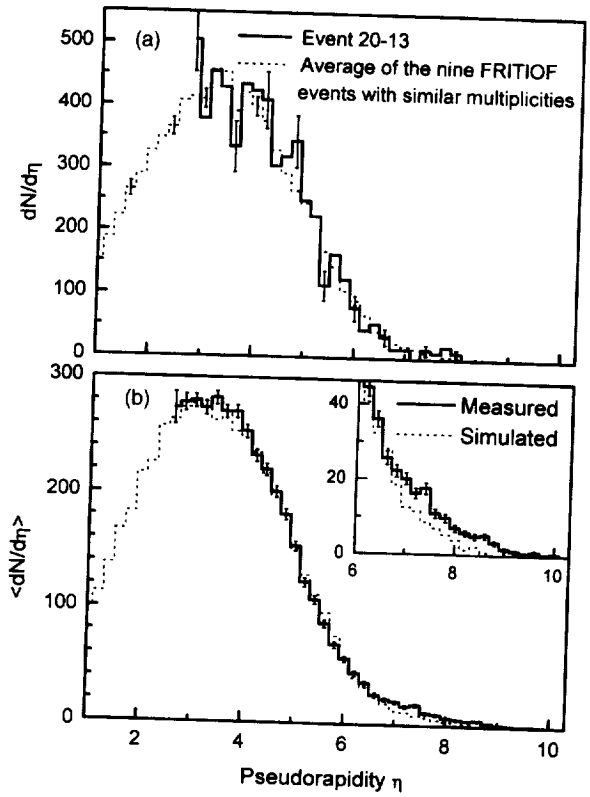

FIG. 2. (a) Pseudorapidity distribution of the highest-multiplicity measured event (solid line), and the average of nine simulated FRITIOF events with similar multiplicities (dotted line). (b) The mean pseudorapidity distribution for the entire measured data sample (solid line) and that for a set of FRITIOF events selected with the same multiplicity distribution as the data (dotted line). Inset shows the region above $\eta=6$ in detail.

The uncertainty in the longitudinal track positions has a statistical component which is greatest at large angles but does not exceed 1%, and an estimated 1% systematic component due to uncertainties in the absolute mechanical spacing between plates during the exposure. The overall uncertainty in the pseudorapidity ranges from ~ 0.01 at small η to 0.03 at $\eta=6$. The value of the pseudorapidity loses significance beyond $\eta=9$.

III. PSEUDORAPIDITY DISTRIBUTIONS

Figure 2(a) shows the pseudorapidity distribution for the single event with the highest multiplicity. In order to compare the data to expectations based on an incoherent superposition model, we have simulated a sample of 1267 ^{208}Pb-Pb collisions using the FRITIOF 7.02 Monte Carlo code [6] with an unrestricted range of impact parameters. In this preliminary study we have run FRITIOF in its default configuration. The dotted curve shows the average pseudorapidity distribution of the nine simulated events with restricted multiplicities $N_{2.9-6}$ within the region $2.9 \leq \eta < 6$ which most closely match that of the measured event. (We base our window on the region above $\eta=2.9$, where all tracks are measured in at least two layers, and below $\eta=6.0$, above which spectators are expected to appear in the measured data. Individual spectators are not included in the FRITIOF calculations.) The two distributions are in good agreement ($\chi^2_\nu=0.83$ over the entire measured range).

TABLE I. Central and semicentral data sets.

Sample	No. events	$\langle N_{Z\geq 2}\rangle$	$\langle N_{\text{prod}}\rangle$
Central	21	0.9 ± 0.8	1314 ± 210
Semicentral	19	5.3 ± 2.2	845 ± 160

The mean pseudorapidity distribution $\langle dN/d\eta\rangle$ for the entire data sample of 40 events is shown in Fig. 2(b) as the solid line. We have matched the measured events with 40 events selected from the FRITIOF set with restricted multiplicities most nearly equal to those of the real events, and have plotted their average distribution as the dotted line. In the region between 2.9 and 6, the difference between the distributions in Fig. 2(b) corresponds to a χ^2 per degree of freedom of 1.33. Again, the shapes of the distributions agree well except for $\eta>6.5$, where the data show the expected contribution by spectators. We note that in Fig. 2(a) the measured and calculated distributions agree well even up to the highest η values. In this most central event, few if any spectators are observed.

To study the shape of the pseudorapidity distribution in the forward cone, we have separated the data set into a "central" sample of 21 events containing two or fewer projectile fragments and a "semicentral" sample comprised of the remaining 19 events (Table I). To compare the shapes of the distributions, we have normalized their areas between $\eta=2.9$ and $\eta=6$ to the area of the mean inclusive distribution, and plotted the normalized distributions for $\eta>6$ in Fig. 3 along with the FRITIOF distribution from Fig. 2(b). The semicentral sample shows a component above the (spectator-free) FRITIOF prediction which is almost completely absent in the central sample, suggesting that FRITIOF predicts the shape of the produced forward distribution reasonably well, and that the "central" sample consists of events in which almost all of the projectile nucleons participate in the interaction.

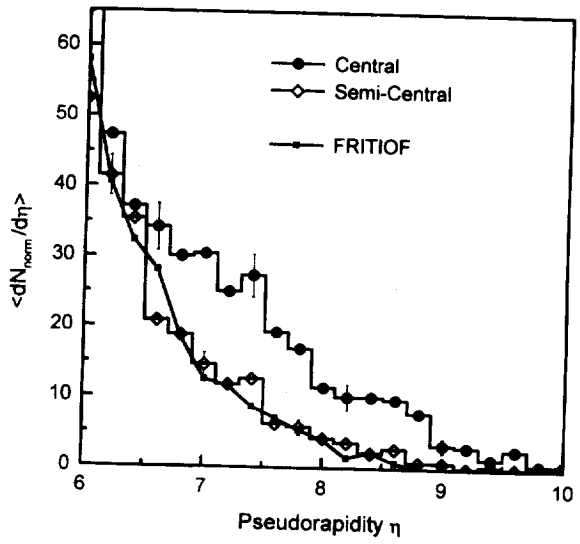

FIG. 3. Comparison of the shapes of the $\eta>6$ region for central, semicentral, and the spectator-free FRITIOF distributions. See text for details.

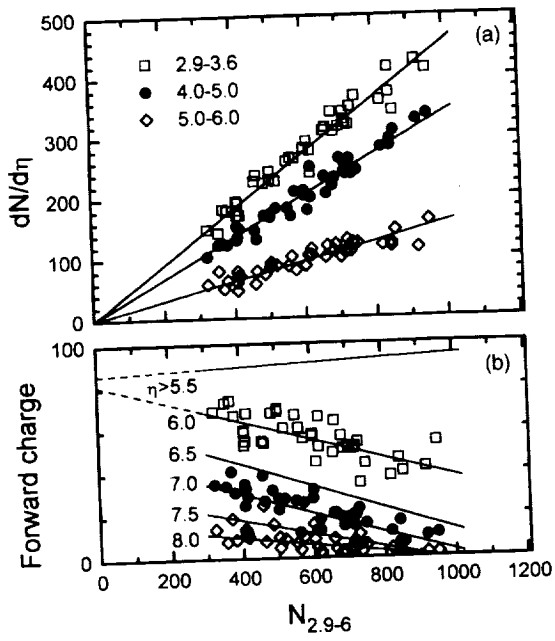

FIG. 4. Relationships of forward charge and multiplicity density to multiplicity for several regions of the pseudorapidity distributions. (a) Produced multiplicities in three intervals. Fits are constrained to pass through the origin. (b) Total charge in several forward cones. The fits are all statistically weighted.

(According to FRITIOF, our central event sample should contain an average of 16 spectator protons distributed over the pseudorapidity range $\eta \geq 6$. We would therefore expect to see an excess of the number of measured tracks above the value for the FRITIOF pions equal to 16. In fact, we see an excess of 2.4 ± 5.0. These values differ by 2.7σ, suggesting that FRITIOF may be overestimating the pion production in the forward direction by perhaps 30%.)

Deviations from the superposition model, if they occur, might be expected to be strongest in the largest events. We look for trends in pseudorapidity shape with changing event size in Fig. 4. In Fig. 4(a) the mean pseudorapidity density appears to be directly proportional to the restricted multiplicity both near the peak and in the forward direction. In particular, there is no indication of a flattening of the central peak even for the high-multiplicity central events. This scaling implies that on average the shapes of the pseudorapidity distributions are independent of the event multiplicity. This linear behavior is reproduced by FRITIOF. Table II compares the one-parameter linear fits shown in Fig. 4 and the corresponding fits to the FRITIOF data. The shapes of the pseudorapidity distributions agree quantitatively with FRITIOF from $\eta = 2.9$ to $\eta = 6.0$ up to the highest measured multiplicities. (The uncertainties in Table II are statistical only. The 5% difference between the measured and the calculated slopes in the $\eta = 5-6$ interval is on the same order as our systematic counting error, and does not appear to be significant.)

TABLE II. Rate of increase of pseudorapidity densities with multiplicity.

Interval	2.9–3.6	4–5	5–6
Data	0.457 ± 0.004	0.340 ± 0.004	0.158 ± 0.003
FRITIOF	0.448 ± 0.001	0.337 ± 0.001	0.167 ± 0.001

Figure 4(b) shows the total (unsigned) charge in five cones centered on the beam axis from $\eta > 5.5$ to $\eta > 8.0$. The fits are shown for all five cones. For clarity, the data from only three representative cones are shown. The forward cones include spectator protons and fragments as well as some produced particles. We have assumed that the fragments are all alphas, and calculated the total charge in the interval accordingly. As Figs. 2 and 3 illustrate, the region forward of $\eta = 6.5$ contains most of the spectator contribution. In this region, increasing the multiplicity (and the centrality) decreases the number of spectators and therefore the total forward charge. Widening the cone to include $\eta > 5.5$ includes enough produced particles so that the charge in this cone increases with increasing multiplicity.

The data in Fig. 4(b) are consistent with a linear relationship between event multiplicity and total charge. An additional test of linearity is possible for the $\eta > 5.5$ and $\eta > 6.0$ cones, which contain essentially all of the spectator charge. Very peripheral events must therefore have a charge of nearly 82 inside these cones. This is what the linear extrapolations predict. Larger cones have charge intercepts that are also consistent with 82.

Summarizing, the pseudorapidity distributions are consistent with superposition in general, and agree well with FRITIOF in particular. The shapes of the distributions are independent of multiplicity. When we compare the shapes of the measured Pb-Pb distributions to the shapes of simulated events with similar multiplicities, we see no significant differences except those in the forward region, which can be attributed to spectators.

IV. MULTIPLICITIES

To estimate the produced charged particle multiplicities (i.e., the multiplicity excluding spectators) over all angles, we have scaled the restricted multiplicity $N_{2.9-6}$ by a factor $N_{\text{prod}}/N_{2.9-6} = 1.82 \pm 0.06$ determined from the FRITIOF sample with $N_{\text{prod}} > 600$ (to mimic our scanning selections). Adding the uncertainty in the scaling factor in quadrature with the estimated systematic uncertainty based on our comparisons of manual and automated reconstructions, we estimate a typical uncertainty in the produced multiplicity of 6%. The produced multiplicity for the largest event [Fig. 2(a)] is then 1729 ± 100.

The multiplicity distribution of our 40 measured events is presented in Fig. 5. We estimate in Sec. II that we have analyzed $(22.2 \pm 2.7)\%$ of all events in the chambers. To make a direct comparison with the data, we calculate the FRITIOF multiplicities using the same prescription $N_{\text{prod}} = 1.82 N_{2.9-6}$ as used to estimate the produced multiplicities of the measured events. (FRITIOF multiplicities computed using the entire η range produce a distribution which is very similar to the one shown, but which falls off somewhat more steeply around 1850.) As expected from our event selection technique, we appear to undersample events with multiplicities less than 1000. At higher multiplicities, there is no evidence for an enhanced production probability. Indeed, we see fewer events above $N_{\text{prod}} = 1400$ than expected. This apparent deficit is statistically unconvincing, but intriguing.

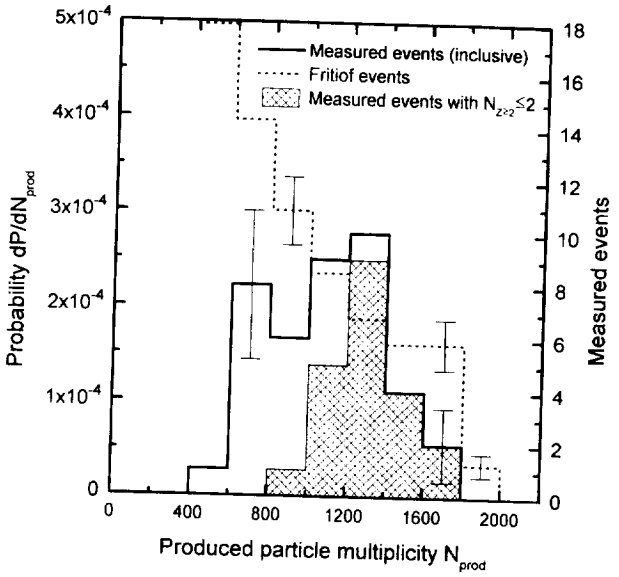

FIG. 5. Probability distribution $dP/dN_{\rm prod}$ of the estimated produced particle multiplicity $N_{\rm prod}=1.82N_{2.9-6}$. The distribution of the data (solid line) has been normalized to an area of 0.222 based on the calculated cross section and event selection efficiencies. The dotted line shows the results from an unbiased FRITIOF sample normalized to an area of unity. The shaded region shows the central events with two or fewer fragments. The right-hand axis shows the number of events in each multiplicity bin.

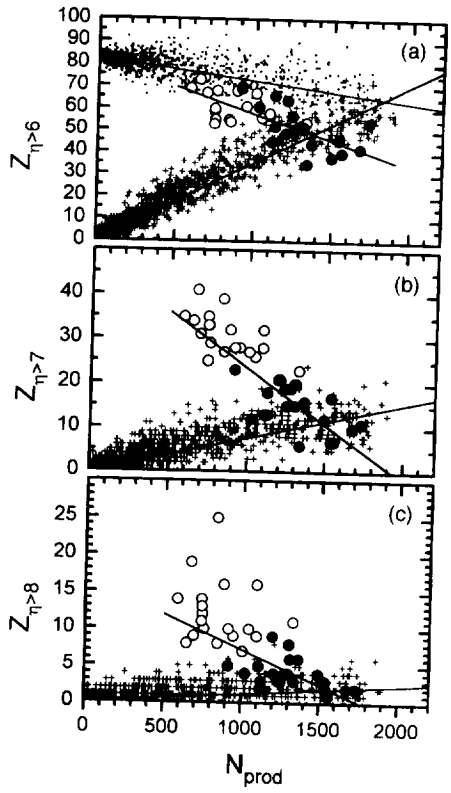

FIG. 6. Measured charge in several forward cones (large solid circles are the central sample; large open circles are the semicentral sample), predicted produced charge (small crosses), and predicted total charge (points in upper band). Note that the vertical scales vary. The straight lines are statistically weighted fits, with the pion base line fit constrained to pass through the origin.

It cannot be fully explained by normalization uncertainties in $N_{\rm prod}$ or our scanning rate.

To further investigate this possible deficit of large events, we examine the spectator region in greater detail. As the impact parameter b decreases to 0, the number of spectators decreases. By using FRITIOF to estimate the number of produced particles in the forward region, we can calculate the multiplicity N_0 corresponding to events with no spectators, i.e., events in which the forward multiplicity is entirely due to produced particles. This multiplicity turns out to be rather insensitive to the FRITIOF model assumptions. Figure 6(a) shows the total charge $Z_{\eta>6}$ in the cone $\eta>6.0$ vs $N_{\rm prod}$. The solid circles represent the central sample with two or fewer fragments, and the large open circles represent the semicentral sample with more than two fragments. Figure 4(b) shows that this cone contains essentially all of the spectator charge. The total charge of the FRITIOF events inside the $\eta>6.0$ cone has therefore been calculated by adding the produced forward multiplicity (the "pion base line," shown as small crosses) to the spectator charge. (FRITIOF does not propagate individual spectators, but does report the total spectator charge.) The FRITIOF calculation of $Z_{\eta>6}$ is displayed as the small points in the top band. The FRITIOF distribution converges to charge 82 on the left, and merges into the pion base line near $N_{\rm prod}=1850$, which a zero impact parameter ($b=0$) run confirms as the mean multiplicity N_0 of head-on events predicted by FRITIOF.

The FRITIOF distribution lies significantly above the measured points. In addition, the $Z_{\eta>7}$ and $Z_{\eta>8}$ distributions in Figs. 6(b) and 6(c) merge into the pion base lines near $N_{\rm prod}=1500$, not near the expected $N_{\rm prod}=1850$. We cannot explain the difference as a systematic counting error or in terms of a bias introduced by our event selection criteria. The intercept of the fit to the measured events at $Z_{\eta>6}=82\pm4$ argues against a large systematic error in fragment charge assignments. In any case, such an error would not greatly effect the central sample, which has an average of only 0.9 fragments per event. We conclude that the discrepancy is real.

The difference indicates that FRITIOF cannot be correctly predicting both N_0 and the pion base line in the forward direction. We first consider the possibility that FRITIOF predicts N_0 correctly and that the difference is entirely due to an incorrect pion base line. If $N_0=1850$ as FRITIOF predicts, one consequence is that our so-called "central" sample is not actually very central, despite the relative lack of alphas and heavier fragments. From Table I, we estimate that these events would have on average $82\times(1850-1314)/1850=24$ spectator protons, equal to the entire mean multiplicity forward of $\eta=6.5$ (25 ± 1). Thus, the produced particle pseudorapidity distribution, which agrees with FRITIOF to within 5% up to $\eta=6.0$, would have to abruptly cut off around $\eta=6.5$, and the tracks forward of $\eta=6.5$ in Fig. 3 would have to be essentially all spectators. Figures 6(b) and 6(c) confirm that for the data to be consistent with $N_0=1850$, an essentially complete absence of produced particles is required in these cones. The agreement in Fig. 3, the deficit in the multiplicity distribution, and the lack of fragments in the central sample all favor the interpretation that the difference between the data and FRITIOF in Fig. 6(a) is not entirely due

TABLE III. Spectator depletion analysis in five forward cones.

Cone	N_0	σ_{stat}	σ_{syst}	$N_0'-N_0$	N_0'	Sensitivity
6.0	1370	60	70	330	1700 ± 340	1.49
6.5	1430	80	70	200	1620 ± 220	0.59
7.0	1480	50	70	120	1600 ± 150	0.31
7.5	1470	60	70	80	1550 ± 120	0.17
8.0	1570	110	80	60	1630 ± 150	0.13

to an incorrect model of the forward region, but is in large measure caused by FRITIOF's overestimate of produced multiplicities.

We now consider the case in which FRITIOF correctly models the forward pseudorapidity distribution, but overestimates the produced multiplicities. In this case, it is possible to estimate the number of spectators in the measured events by subtracting the pion base line. The mean multiplicity N_0 of head-on events, which have almost no spectators, is then estimated by the intersection in Fig. 6 of the fits to the measured events and to the pion base line. (For simplicity, we neglect the small correction due to the fact that even head-on events probably have an estimated four charged spectator nucleons. This causes us to slightly overestimate N_0.) FRITIOF's total charge distribution in Fig. 6(a) crosses the produced particle line at 1840, which agrees well with the direct calculation of $N_0=1850$, demonstrating the reliability of the analysis technique. The analysis has been applied in five cones from $\eta>6.0$ to $\eta>8.0$, and the results are summarized in the second column of Table III.

As discussed in Sec. III, FRITIOF may actually overestimate the forward production by an amount on the order of 30%, in which case the pion base line slopes in Fig. 6 are too steep, and the values of N_0 calculated in Table III are slightly too low. Table III also gives a corrected value N_0' of the head-on multiplicity in the case where the slope m of the pion base line is decreased by 30%.

The systematic error σ_{syst} in N_0 is dominated by the uncertainty in N_{prod}. There is also an uncertainty in the fragment charge assignment which propagates into N_0, but this contribution turns out to be negligible. Even assuming that the fragments are all carbon only changes the value of N_0 by 40: The intersection is mainly determined by the fragment-poor central points near the pion base line. The systematic uncertainty due to the uncertainty in the forward production can be estimated from $N_0'-N_0$. Combining the statistical and systematic uncertainties, we find values of N_0' from the five cones ranging from 1550 ± 120 to 1700 ± 340, all smaller than the FRITIOF value of 1850.

The sensitivity

$$\frac{\Delta N_0/N_0}{\Delta m/m}$$

of N_0 to the pion base line slope m can be reduced as shown in Table III by choosing a narrow cone. However, the statistical uncertainty increases as the cone is restricted. We choose the $\eta>7.5$ cone as the best compromise. Our best value of N_0' is then 1550 ± 120. The smallest that the pion base line slope can possibly be is 0 ($\Delta m/m=-1$), corresponding to no pions at all in the $\eta>7.5$ cone. In this case, the head-on multiplicity would rise to 1730, still below the FRITIOF value of 1850.

Finally, we combine our multiplicity and pseudorapidity results to find a relationship between multiplicity and peak pseudorapidity density. We use the data from the $\eta=2.9-3.6$ interval in Fig. 4 along with the factor of 1.82 from FRITIOF to quantify the relationship between produced multiplicity and $\langle dN/d\eta\rangle$ at the peak of the pseudorapidity distribution. The best linear fit (constrained to pass through the origin) gives $\langle dN_{prod}/d\eta\rangle_{peak}=(0.25\pm0.01)\times N_{prod}$. Thus the mean pseudorapidity density for $b=0$ events should be 390 ± 30. The highest pseudorapidity density we observe in a particular event is 425.

Summarizing, our study of event multiplicities shows a significant difference from FRITIOF when the forward charges are compared to the event multiplicities. Our estimate of the mean multiplicity of head-on events N_0' is 1550 ± 120, corresponding to a mean peak pseudorapidity density of 390 ± 30. No matter what the forward distribution, the best estimate of 1550 cannot increase to more than 1730, corresponding to $\langle dN/d\eta\rangle_{peak}=430$.

V. DISCUSSION

Comparison of the data to FRITIOF shows good agreement in the pseudorapidity distributions at pseudorapidity densities as high as 425. There is no evidence in the data for flattening of the central pseudorapidity peak, even at pseudorapidity densities 6 times higher than in experiments at similar energies (200 GeV/nucleon O and S on emulsion [7]). Such flattening might be expected if a quark-gluon plasma had been formed [2]. It should be noted, however, that even for the largest event, with a central pseudorapidity density of 425, assuming $\langle p_{t\pi}\rangle=350$ MeV/c (FRITIOF value) and an interaction distance $2ct=2$ fm/c, the energy density evaluated with the standard expression [1] from Bjorken's model,

$$\epsilon=\frac{3}{4\pi A^{2/3}t}(\langle p_{t\pi}\rangle^2+m_\pi^2)^{1/2}\frac{dN}{d\eta}$$

(where $A=208$ is the mass number), corresponds[1] to only 1.1 GeV fm^{-3}. Although this energy density is significantly higher than in previous experiments at similar energy, it may still be below the point at which a quark-gluon plasma should be formed.

Our determination of the mean multiplicity of head-on events, $N_0'=1550\pm120$, is significantly lower than the value that FRITIOF predicts. It should be noted, however, that Adamovich *et al.* [8] report FRITIOF simulations with a mean production rate of 7.68 particles per nucleon-nucleon collision, implying $N_0=208\times7.68=1600$, in agreement with our measurements. The suggestion that these events are smaller than FRITIOF predictions has also been made by the EMU-01 Collaboration based on the analysis of their first two events

[1]There is a great deal of uncertainty in this number [1]. NA49 [9] uses a prescription which gives an energy density about twice as high as cited here, mainly because the formation times differ by a factor of 2.

[10]. The first results of the NA49 experiment [9] showed a peak negative particle multiplicity $dN_-/d\eta = 230$ for central events, indicating a charged particle multiplicity density of 460. This is higher than our value but perhaps consistent with it.

The value of N_0' marks the beginning of the tail of the multiplicity distribution. In the superposition model, the width of this tail is determined by the width of the p-p multiplicity distribution and the statistics of 208 independent nucleon-nucleon collisions. FRITIOF predicts the standard deviation of the $b=0$ multiplicity distribution to be 60. If Pb-Pb interactions are indeed simply the result of independent nucleon-nucleon interactions, then with better statistics one would expect to see a rather rapidly diminishing tail beyond N_0' with a width of approximately 60.

Although the method used to determine N_0' requires a model of the pion base line, it has some noteworthy compensatory advantages that distinguish it from other techniques. It does not rely on multiplicity cuts which could bias the result. (Figure 5 distinguishes the central and semicentral samples used in Sec. III, but the entire data set is used in the multiplicity analysis.) It is insensitive to sampling biases, and does not require that the tail of the distribution be fully sampled. The result is almost independent of the absolute calibration of the forward charge measurement. And it can be performed with a small set of carefully measured events in which the tracks have been individually counted.

In conclusion, charged particle multiplicities and pseudorapidity distributions have been measured by counting individual tracks in a sample of 40 high-multiplicity Pb-Pb collisions. The shapes of the pseudorapidity distributions are in good agreement with the results expected from calculations based on a superposition model of individual nucleon-nucleon collisions. Despite calculated energy densities twice those of previous experiments, we see no indication of QGP formation in the form of flattened pseudorapidity distributions or enhanced multiplicities. Indeed, our best estimate of the mean multiplicity of zero impact parameter events is 1550 ± 120, about 16% lower than predicted by FRITIOF.

ACKNOWLEDGMENTS

This work was partially supported in the U.S. by the National Science Foundation (Grants Nos. PHY-921361 and INT-8913051 at LSU) and Department of Energy (Grant No. DOE-FG02-89ER40528 at Minnesota), and in Poland by State Committee for Scientific Research Grant No. 2P03B18409 and Maria Sklodowska-Curie Fund II No. PAA/NSF-96-256. P.D. thanks the Louisiana State Board of Regents (LEQSF) under agreements Nos. NASA/LSU-91-96-01 and NASA/ LaSPACE under Grant No. NGT-40039 for its support. Construction of the automated microscope system was funded by NASA (Grants Nos. NAGW-3289 and NAGW-3560) at LSU. We very much appreciate the help of the CERN staff, A. Aranas and J. Dugas at LSU, and especially Professor Y. Takahashi and his EMU-16 colleagues for their generous assistance.

[1] H.R. Schmidt and J. Schukraft, J. Phys. G **19**, 1705 (1993).
[2] J.D. Bjorken, Phys. Rev. D **27**, 140 (1983).
[3] B.S. Nilsen, C.J. Waddington, J.R. Cummings, T.L. Garrard, and J. Klarmann, Phys. Rev. C **52**, 3277 (1995).
[4] L.Y. Geer, J. Klarmann, B.S. Nilsen, C.J. Waddington, W.R. Binns, J.R. Cummings, and T.L. Garrard, Phys. Rev. C **52**, 334 (1995).
[5] P. Deines-Jones, M.L. Cherry, W.V. Jones, K. Sengupta, T. Tominaga, and J.P. Wefel, Proceedings of the 23rd International Cosmic Ray Conference, Calgary, 1993, Vol. 2, p. 536.
[6] H. Pi, Comput. Phys. Commun. **71**, 173 (1992).
[7] A. Dabrowska *et al.*, Phys. Rev. D **47**, 1751 (1993).
[8] M.I. Adamovich *et al.*, Phys. Rev. Lett. **69**, 745 (1992).
[9] S. Margetis *et al.*, Nucl. Phys. **A590**, 355c (1995).
[10] E. Stenlund *et al.*, Nucl. Phys. **A590**, 597c (1995).